Supporting Information

Three-Dimensional Hierarchical Porous Structure Constructed by Two-Stage MXene-Wrapped Si Nanoparticles for Li-Ion Batteries

Xin Li, Zhiyu Chen, Ang Li, Yingchun Yu, Xiaohong Chen ,and Huaihe Song**

State Key Laboratory of Chemical Resource Engineering, Beijing Key Laboratory of Electrochemical Process and Technology for Materials, Beijing University of Chemical Technology, Beijing 100029, P. R. China

*Corresponding author E-mail: chenxh@mail.buct.edu.cn

songhh@mail.buct.edu.cn

Figure S1. Physical photos of SiNP and MXene electrostatic self-assembly under different pH conditions.

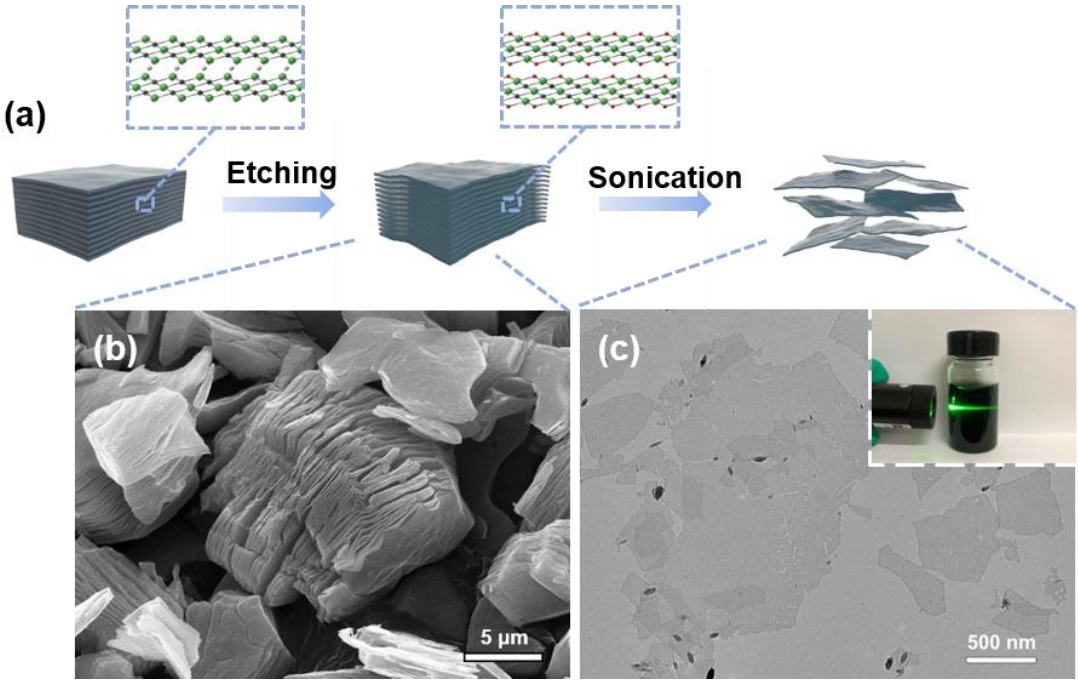

Figure S2. (a) Schematic illustration of the synthesis process of MXene nanosheets. (b) SEM image after Ti_3AlC_2 etching. (c)TEM image of MXene nanosheets.

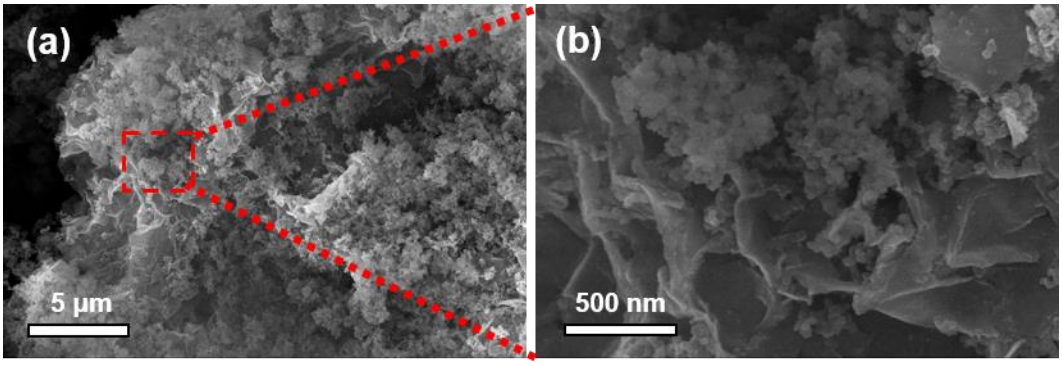

Figure S3. (a, b) SEM images of SiNP@MX2 under different magnifications.

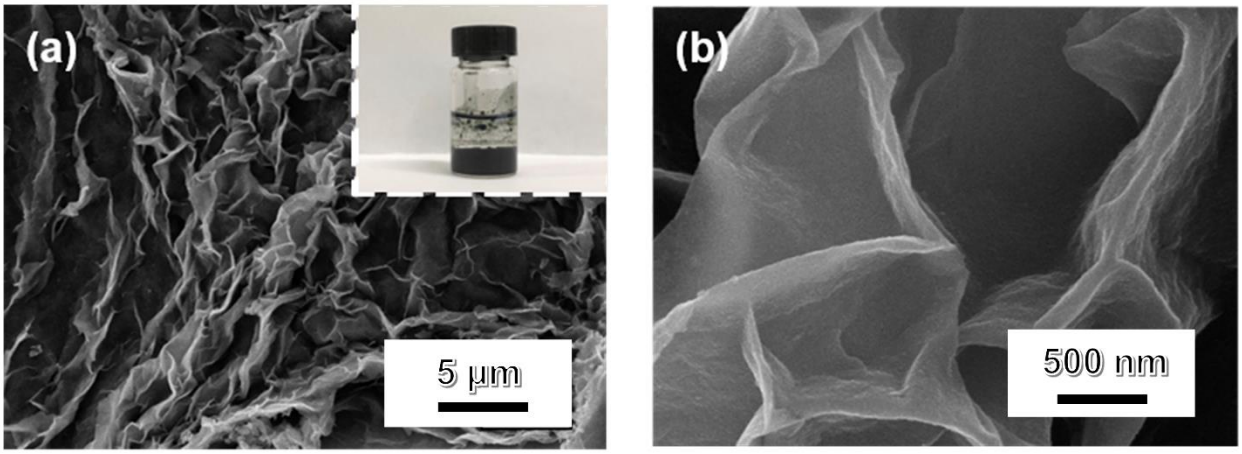

Figure S4. (a) SEM image and physical photo of 3D porous MXene skeleton. (b) SEM image at high magnification.

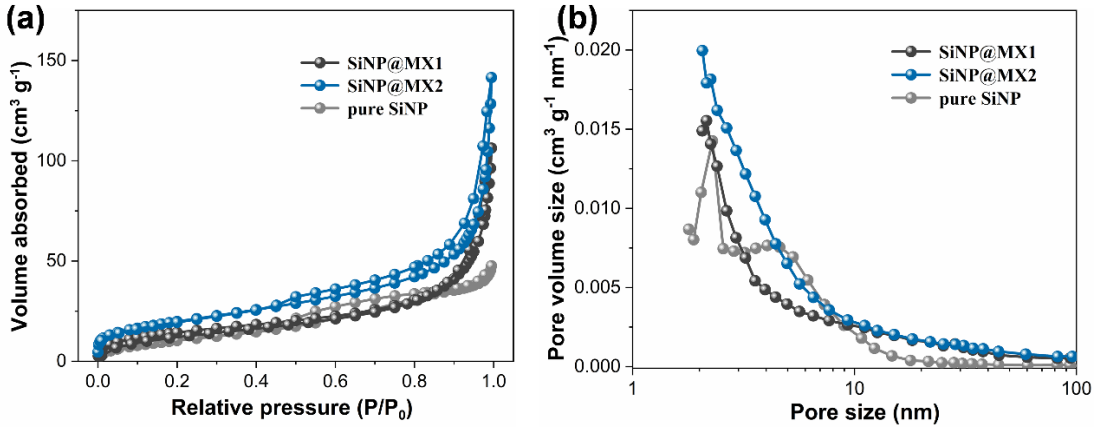

Figure S5. (a) N_2 adsorption-desorption isotherm and (b) pore-size distribution curves of pure SiNP, SiNP@MX1 and SiNP@MX2.

Table S1. Specific surface area and pore analyses of pure SiNP, SiNP@MX1, SiNP@MX2 as well as SiNP@MX1/MX2.

Sample	BET Surface area (m^2 g^{-1})	Pore volume (cm^3 g^{-1})	BJH Desorption average pore diameter (nm)
SiNP	41.01	0.066	5.4
SiNP@MX1	52.44	0.153	15.4
SiNP@MX2	71.62	0.210	12.3
SiNP@MX1/MX2	90.17	0.362	20.4

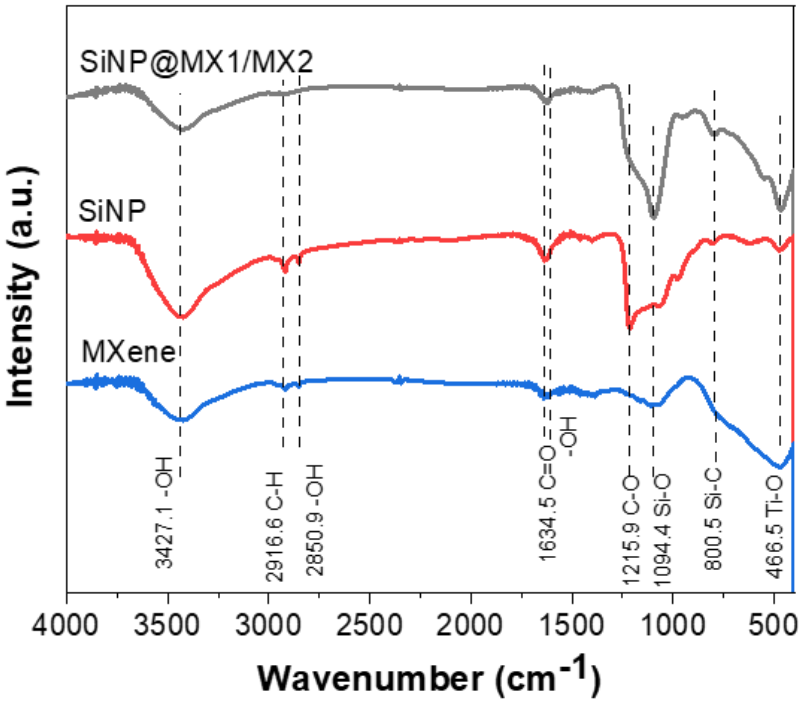

Figure S6. FT-IR spectra of SiNP@MX1/MX2, SiNP and MXene.

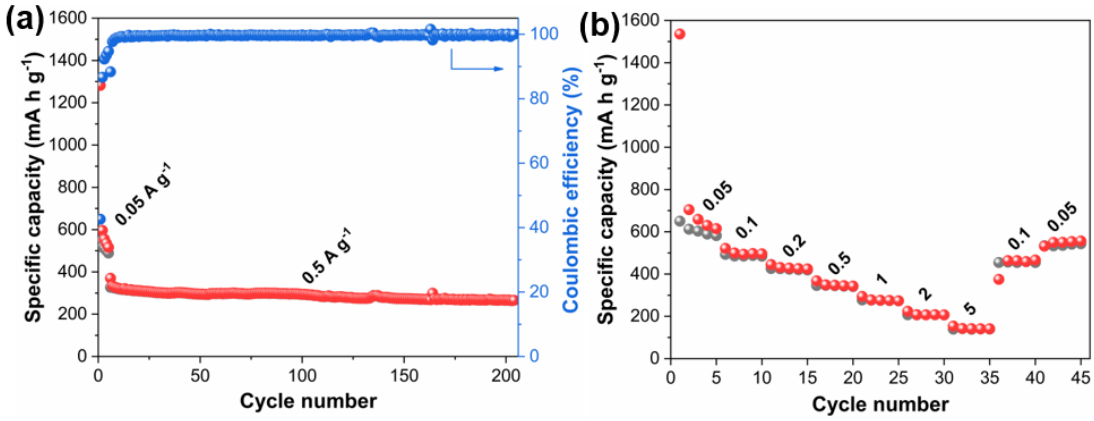

Figure S7. Electrochemical performance of 3D porous MXene skeleton. (a) Long-term cycling performance in a cyclic current density of 0.5 A g^{-1}. (b) Rate capability at various current densities from 0.05 Ag^{-1} to 5.0 A g^{-1}.

Table S2. Mass ratio of major elements in MXene samples calculated by XPS.

Element	Atomic ratio (%)	Mass ratio (wt.%)
C	53.98	34.74
O	22.25	19.08
Ti	14.30	36.68
F	8.93	9.09
N	0.54	0.40

Table S3. Mass ratio of major elements in SiNP@MX1/MX2 samples calculated by XPS.

Element	Atomic ratio (%)	Mass ratio (wt.%)
C	36.22	24.80
O	43.37	39.56
Ti	3.17	8.66
Si	16.28	26.07
F	0.55	0.59
N	0.40	0.32

Table S4. Comparison of electrochemical performance of SiNP@MX1/MX2 anode with other Si-based anodes reported recently.

	Sample	ICE (%)	Current density ($A\ g^{-1}$)	Capacity ($mAh\ g^{-1}$)	Cycle number	Retention	References
1	***SiNP@MX1/MX2***	***67.2%***	***0.5***	***1422***	***200***	***89.7%***	***This work***
2	GNS@OLC-Si	79.46%	0.5	1129.3	300	72.1%	[1]
3	Si@GC	78.6%	0.5	1450.7	400		[2]
4	m-Si@G	53%	1	483	600	70.8%	[3]
5	Si@Ti_3C_2	69%	0.2	188	150	21.4%	[4]
6	Si@Ti_3C_2 (8:2)	58.6%	1	1342.8	200		[5]
7	MXene&Si	61%	0.5	252	200		[6]
8	Si@MXene	74.7%	0.5	1003.6	150	81.0%	[7]
9	Si p-NS@TNSs	80.2%	0.2	1154	150	55.6%	[8]
10	Ti_3C_2/Si	61.1%	0.1	1475	150		[9]

Table S5. Corresponding to the resistance value of the equivalent circuit.

Samples	Rs(Ω)	RSEI(Ω)	Rct(Ω)
pure SiNP	1.1	-	518.3
pure SiNP (200th)	3.1	1061	1879
SiNP@MX1/MX2	2.6	-	142.4
SiNP@MX1/MX2 (200th)	3.7	4.5	62.6

References

1. Wang, D.; Zhou, C.; Cao, B.; Li, A.; Chen, X.; Yang, R.; Song, H., Construction of a secondary conductive and buffer structure towards high-performance Si anodes for Li-ion batteries. *Electrochim. Acta* **2020,** *354*, 136767.

2. Wang, H.; Ding, Y.; Nong, J.; Pan, Q.; Qiu, Z.; Zhang, X.; Zheng, F.; Wu, Q.; Huang, Y.; Li, Q., Bifunctional NaCl template for the synthesis of Si@graphitic carbon nanosheets as advanced anode materials for lithium ion batteries. *New J. Chem.* **2020,** *44* (33), 14278-14285.

3. Gao, R.; Tang, J.; Yu, X.; Zhang, K.; Ozawa, K.; Qin, L.-C., A green strategy for the preparation of a honeycomb-like silicon composite with enhanced lithium storage properties. *Nanoscale* **2020,** *12* (24), 12849-12855.

4. Kong, F.; He, X.; Liu, Q.; Qi, X.; Sun, D.; Zheng, Y.; Wang, R.; Bai, Y., Enhanced reversible Li-ion storage in Si@Ti_3C_2 MXene nanocomposite. *Electrochem. Commun.* **2018,** *97*, 16-21.

5. Yang, Q.; Wang, Z.; Xia, Y.; Wu, G.; Chen, C.; Wang, J.; Rao, P.; Dong, A., Facile electrostatic assembly of Si@MXene superstructures for enhanced lithium-ion storage. *J. Colloid Interface Sci.* **2020,** *580*, 68-76.

6. Li, H.; Lu, M.; Han, W.; Li, H.; Wu, Y.; Zhang, W.; Wang, J.; Zhang, B., Employing MXene as a matrix for loading amorphous Si generated upon lithiation towards enhanced lithium-ion storage. *J. Energy Chem.* **2019,** *38*, 50-54.

7. Yan, Y.; Zhao, X.; Dou, H.; Wei, J.; Sun, Z.; He, Y.-S.; Dong, Q.; Xu, H.; Yang, X., MXene Frameworks Promote the Growth and Stability of LiF-Rich Solid–Electrolyte Interphases on Silicon Nanoparticle Bundles. *ACS Appl. Mater. Interfaces* **2020,** *12* (16), 18541-18550.

8. Xia, M.; Chen, B.; Gu, F.; Zu, L.; Xu, M.; Feng, Y.; Wang, Z.; Zhang, H.; Zhang, C.; Yang, J., $Ti_3C_2T_x$ MXene Nanosheets as a Robust and Conductive Tight on Si Anodes Significantly Enhance Electrochemical Lithium Storage Performance. *ACS Nano* **2020,** *14* (4), 5111-5120.

9. Hui, X.; Zhao, R.; Zhang, P.; Li, C.; Wang, C.; Yin, L., Low-Temperature Reduction Strategy Synthesized Si/Ti_3C_2 MXene Composite Anodes for High-Performance Li-Ion Batteries. *Adv. Energy Mater.* **2019,** *9* (33), 1901065.